Geodinamica Acta

Geodinamica Acta 19/5 (2006) 265-280

$^{40}Ar/^{39}Ar$ geochronology constraints on the Middle Tertiary basement extensional exhumation, and its relation to ore-forming and magmatic processes in the Eastern Rhodope (Bulgaria)

Nikolay Bonev [a]* , Peter Marchev [b], Brad Singer [c]

[a] *Department of Geology and Paleontology, Faculty of Geology and Geography, Sofia University "St. Kliment Ohridski", 15 Tzar Osvoboditel Bd., 1504 Sofia, Bulgaria*

[b] *Geological Institute, Bulgarian Academy of Sciences, Acad. G. Bonchev St.,Bl.24., 1113 Sofia, Bulgaria*

[c] *Department of Geology and Geophysics, University of Wisconsin-Madison, 1215 West Dayton St., Madison, WI 53706, USA*

Received: 22/12/03, accepted: 07/12/04

Abstract

The interaction of distinct geologic processes involved during late orogenic extensional exhumation history of the metamorphic units in the Eastern Rhodope is refined by new and reviewing $^{40}Ar/^{39}Ar$ geochronological and structural data. Minerals with different closure temperatures from metamorphic rocks investigated in this study are combined with those from magmatic and ore-forming hydrothermal rocks in two late stage metamorphic domes – the Kesebir-Kardamos and the Biala reka-Kehros domes. The 38-37 Ma muscovite and biotite cooling ages below 350°-300°C characterize basement metamorphic rocks that typified core of the Kesebir-Kardamos dome, constraining their exhumation at shallow crustal levels in the footwall of detachment. These ages are interpreted as reflecting last stage of ductile activity on shear zone below detachment, which continued to operate under low-temperature conditions within the semi-ductile to brittle field. They are close to and overlap with existing cooling ages in southern Bulgaria and northern Greece, indicating supportively that the basement rocks regionally cooled between 42-36 Ma below temperatures 350°-300°C. The spatial distribution of ages shows a southward gradual increase up structural section, suggesting an asymmetrical mode of extension, cooling and exhumation from south to the north at latitude of the Kesebir-Kardamos dome. The slightly younger 36.5-35 Ma crystallization ages of adularia in altered rocks from the ore deposits in the immediate hanging-wall of detachments are attributed to brittle deformation on high-angle normal faults, which further contributed to upper crustal extension, and thus constraining the time when alteration took place and deformation continued at brittle crustal levels. Silicic dykes yielded ages between 32-33 Ma, typically coinciding with the main phase of Palaeogene magmatic activity, which started in Eastern Rhodope region in Late Eocene (Priabonian) times. The $^{40}Ar/^{39}Ar$ plateau ages from the above distinct rock types span time interval lasting approximately ca. 6 Ma. Consequently, our geochronologic results consistently indicate that extensional tectonics and related exhumation and doming, epithermal mineralizations and volcanic activity are closely spaced in time. These new $^{40}Ar/^{39}Ar$ age results further contribute to temporal constraints on the timing of tectonic, relative to ore-forming and magmatic events, suggesting in addition that all above mentioned processes interfered during the late orogenic extensional collapse in the Eastern Rhodope region.

Keywords: $^{40}Ar/^{39}Ar$ geochronology, extensional tectonics, magmatism, ore deposits, Rhodope, Bulgaria

* Corresponding author.
Tel: +3592 9308 431 - *Fax*: +3592 944 64 87
E-mail address: niki@gea.uni-sofia.bg

1. Introduction

Recent advance in the study of structural and metamorphic evolution of metamorphic terrains and dating their exhumation history in the north Aegean domain of the Eastern Mediterranean region, has shown distinct tectonometamorphic episodes of thrust imbrication and subsequent crustal thinning through extension during distinct times [1–8]. Preservation of pre-Alpine ages [7, 9, 10], and continuous Alpine geochronologic record from at least late Early Cretaceous with ages gradually decreasing well into the Eocene to Miocene [10–13] demonstrate a protracted cooling history of the accretionary orogenic wedge along the convergent Eurasian plate margin, possibly in a predominant extensional environment during the late orogenic evolution. This tectonic setting includes an early stage of syn-to post-thickening extension as well as late post-orogenic Aegean back-arc extension. A large number of above geochronologic studies on the Greek part of the Rhodope metamorphic province have shed light on the temporal evolution of tectonic and metamorphic events during the Alpine orogeny [10–12]. However, the timing of extensional exhumation of the Rhodope metamorphic province in Bulgaria remains generally less well constrained due to the lack of sufficient and precise age determinations. Generally, the tectonic and magmatic processes are tightly involved during the extensional collapse of orogens [5, 14–16]. Therefore, refining cooling history of metamorphic terrains and its connection with mineralization and magmatic events during crustal extension is important to better understanding of temporal evolution of exhumation process within the Alpine orogen in the northernmost Aegean domain.

We focus our attention on the eastern Rhodope area in Bulgaria, where crustal extension and associated processes of magmatism and mineralization are best portrayed. Two key areas are considered in this study, including the Kesebir-Kardamos and the Biala reka-Kechros domes with ore deposits located within or along their borders. In this paper we present new $^{40}Ar/^{39}Ar$ geochronologic data from the basement gneiss. The new data will be combined with the results for the igneous rocks and hydrothermal mineralization from a companion paper [17] and recently published data from the metamorphic basement [10, 13] to evaluate temporal relationships between the distinct processes. These results are combined with analysis of field data and structural relationships that can yield understanding of evolution of deformation during exhumation processes of mid-crustal level metamorphic rocks.

The major goals of the present paper are: (i) to refine cooling history of high-grade metamorphic rocks. We examine spatial variations in that cooling history in the flanks of the Kesebir-Kardamos dome for the better understanding the timing of exhumation of amphibolite facies rocks; (ii) to decipher whether ore-forming processes and magmatic activity were coeval with extensional doming and whether they share different or overlapping cooling/crystallization histories; and (iii) to discuss $^{40}Ar/^{39}Ar$ results from the metamorphic rocks facing their exhumation history together with those from the igneous and hydrothermally altered rocks, which may provide a window for the thermochronological evolution in the Eastern Rhodope region, both in South Bulgaria and Northern Greece.

2. Geological framework

2.1. General setting

The Rhodope metamorphic province, outcropping mainly in southern Bulgaria and northern Greece, is regarded to be the most internal zone in this sector of the Alpine-Himalayan orogenic system in the Eastern Mediterranean region (Fig. 1). It results from the tectonic history related to the Cretaceous-Recent subduction and convergent setting along the active Eurasian plate margin [18, 19]. The Mid-Cretaceous convergence between Africa and Eurasia was responsible for the growing Rhodope Massif as a crustal-scale metamorphic wedge paired with the Vardar olistostromic trench [20]. Syn-metamorphic thrusting and crustal thickening in the convergent region involved both coeval and subsequent extension [2]. Generally, the Rhodope metamorphic province consists of high-grade metamorphic basement (mainly amphibolite facies) intruded by Late Cretaceous to Mid-Tertiary plutonic rocks [21–23]. Voluminous felsic and basic, Eo-Oligocene volcanics [16, 24, 25] and Late Cretaceous/Early Tertiary to Pliocene sediments [26, 27] cover the crystalline basement.

2.2. Regional geology of the Eastern Rhodope region

The eastern Rhodope region in Bulgaria and Greece (Fig. 1) exposes tectonometamorphic complexes, which are characterized by different metamorphic P-T history and geochronologic ages [28], separated by tectonic contacts of predominant extensional origin [29]. In Bulgaria, they are represented by gneiss-migmatite complex as lowermost structural unit, and an overlying variegated complex of mixed meta-sedimentary and meta-igneous protoliths as an upper structural unit. These metamorphic complexes represent the lower and upper plate rocks of the extensional low-angle detachment fault systems. The subdivision of the metamorphic pile and its equivalents in Greece, adopted here for the sake of simplicity, into a lower tectonic unit (gneiss-migmatite complex, and the Kardamos and Kechros complexes as equivalents) and an upper tectonic unit (variegated complex, and the Kimi Complex as equivalent) is based mainly on structural information. They represent corresponding parts of regionally extensive intermediate thrust sheets and upper units of the Rhodope thrust system [2], respectively, and broadly correlate with the metamorphic sequence in the studied area in Bulgaria. The upper tectonic unit comprises interlayered amphibolites, marbles, various schists and gneisses enclosing eclogite lenses and meta-ophiolites. The lower tectonic unit is composed of para- and predominant ortho-gneisses, and migmatitic gneisses intercalated, at different stratigraphic levels, with schists and amphibolites.

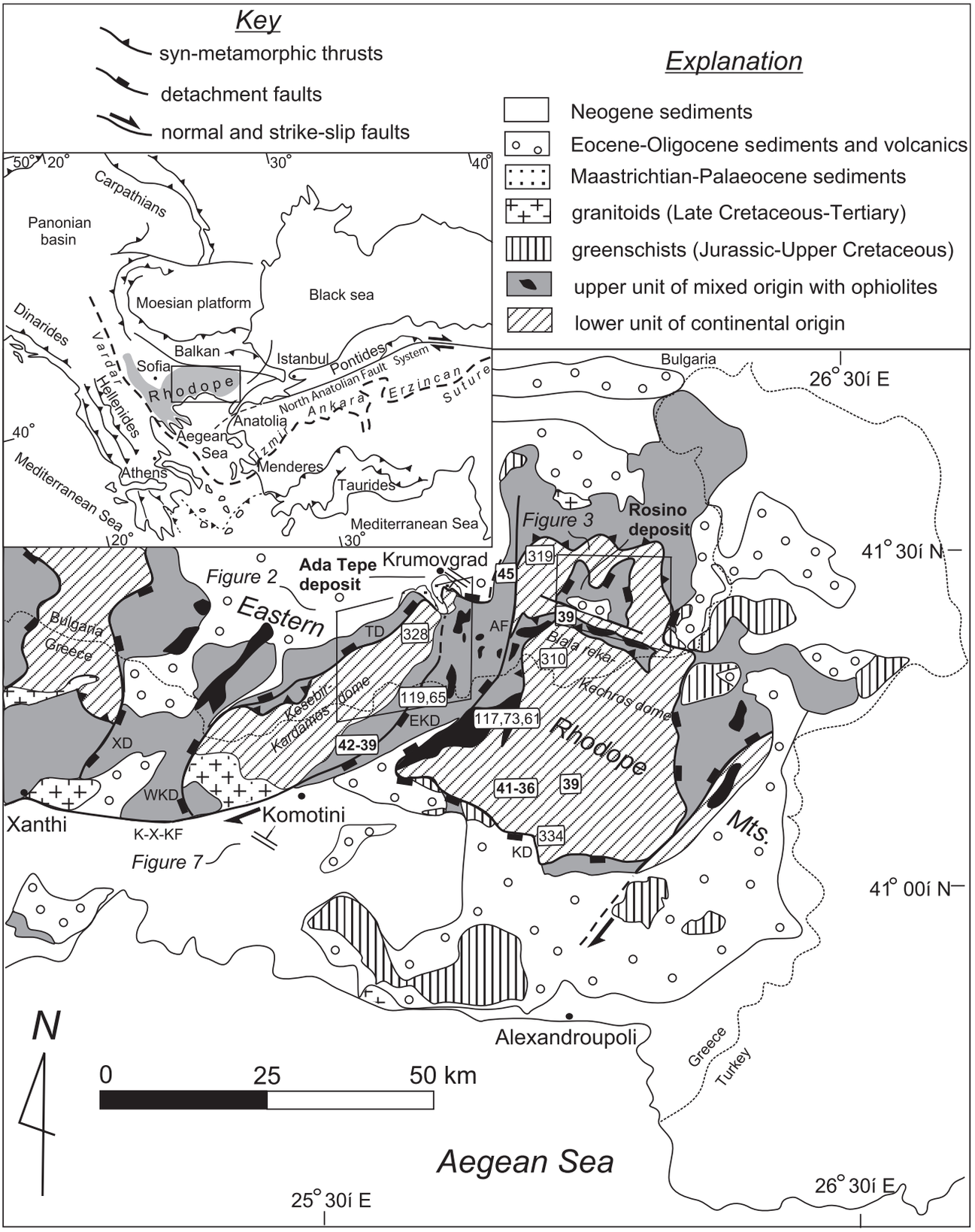

Figure 1: Simplified tectonic map of the eastern Rhodope region in Bulgaria and Greece (adapted from [2, 29] and own data), showing the main tectonic units. Boxes represent locations and ages of published geochronologic data referred to in the text. K-Ar and $^{40}Ar/^{39}Ar$ ages are indicated with thick numbers. Inset: location of the Rhodope Massif in a framework of the Alpine collisional system in the Eastern Mediterranean. Abreviations: **WKD**= West Kardamos detachment, **EKD**= East Kardamos detachment, **KD**= Kechros detachment, **TD**= Tokachka detachment, **XD**= Xanthi detachment, **K-X-KF**= Kavala-Xanthi-Komotini fault, **AF**= Avren fault

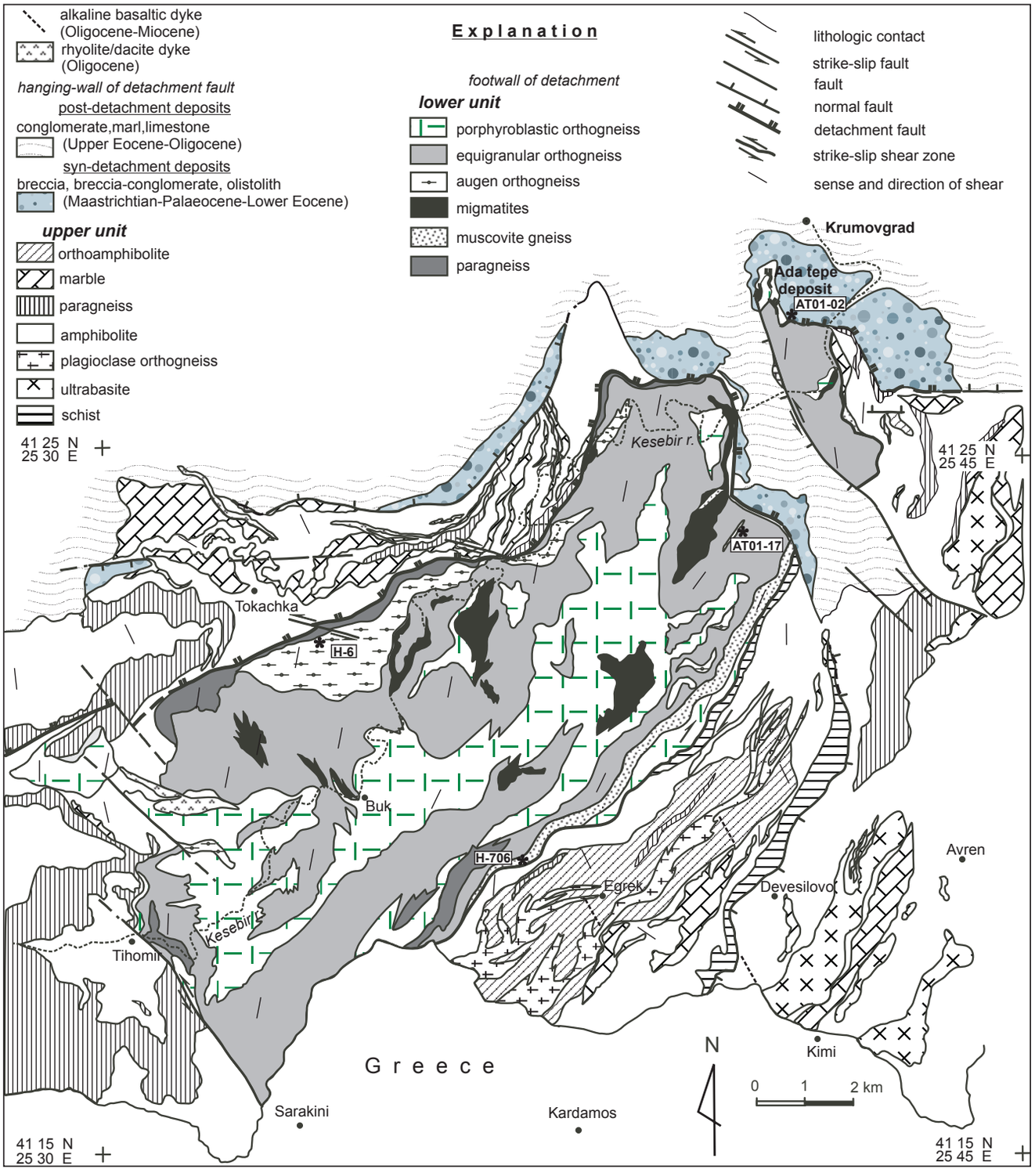

Figure 2: Simplified geological map of the Kesebir-Kardamos gneiss dome (after [46]), showing generalized kinematic pattern and location of samples used for the $^{40}Ar/^{39}Ar$ geochronology.

High-pressure eclogite facies, followed by medium-pressure amphibolite facies and late greenschist facies metamorphism are generally recognized as the major metamorphic events [30]. The high-pressure/high-temperature eclogite/granulite facies conditions in the upper unit (Kimi Complex) at P~13.5-16 kbar and T~750-775 ºC, decreased to 10.5 kbar and 630 ºC in medium-pressure event, subsequently retrogressed into the greenschist facies [28]. Slightly lower P-T estimates (10-12 kbar and 440-520 ºC) for the high-pressure event have been obtained in variegated complex, analogous to the Kimi Complex, on the Bulgarian side [13]. Locally, an earliest ultrahigh-pressure conditions > 26 kbar and above 900 ºC in

the same unit are indicated by diamond and coesite inclusions in garnets [31]. The lower unit (Kardamos Complex) records maximum pressures of 13-16 kbar for an assumed temperature of 600 ºC, followed by amphibolite facies overprint at pressure < 8 kbar and temperatures of 560-620 ºC [28]. In Greece, the eclogite facies metamorphism of the Kechros Complex in the lower tectonic unit occurred at 14-15 kbar and ~550 ºC, followed by medium-pressure upper greenschist to lower amphibolite facies overprint at 4 kbar [30]. The P-T path of the lower unit is characterized by nearly isothermal decompression.

Sedimentary basins and numerous fault-bounded half grabens, containing relatively thick sedimentary sequences of continental clastic, marine and volcaniclastic deposits, ranging in age from Maastrichtian-Palaeocene, Eocene to Miocene, are an important feature of the geology of the eastern Rhodope [26, 27]. They form a supracrustal unit spatially linked to metamorphic domes, located in the hanging wall of presently low-angle detachments, and thus, provide sedimentary constraints on the onset and progression of crustal extension. The widespread Eocene-Oligocene volcanism, developed in several volcanic areas coeval or subsequent to sedimentary basin formation, is dominated by intermediate to acid lavas and associated volcaniclastic products, and subordinate basic varieties [16, 24, 32]. It is considered as collision-related [25, 33], but late tensional dykes swarms that fed the lava flows may indicate that volcanism continued in post-collisional tectonic setting [16]. Numerous dykes of intra-plate basalts located in the two domes terminate magmatic activity in the area [16, 34].

2.3. Previous geochronologic data on the tectonometamorphic and magmatic events

Variscan ages of gneiss-migmatite complex obtained by U-Pb zircon dating of orthogneisses range between 319-305 Ma [9], which are supported by the 334 Ma Rb-Sr isochron age of a metapegmatite [35] in the Biala reka-Kechros dome, and 328 Ma Rb-Sr whole-rock data of an orthogeneiss from the Kesebir-Kardamos dome [36]. Similar ages were recognized also in Serbo-Macedonian and Pelagonian zones to the south in Greece [7, 8, 10]. The age of the high-pressure metamorphism in the Kimi Complex is indicated by the 119 Ma Sm-Nd isochron from a garnet pyroxenite [37], although a similar 117 Ma U-Pb SHRIMP age of zircon core domains in another garnet pyroxenite is interpreted as protolith age. The zircon rims yielded an age of 73 Ma for the high-pressure metamorphism, and 61 Ma for the greenschist facies overprint [38]. The latter ages are consistent with the time of emplacement (69 Ma, Marchev *et al*. unpubl. data) of some granitoids in the Biala reka-Kechros dome and with a 65 Ma Rb-Sr muscovite age from a pegmatite, constraining the timing of the medium-pressure event in the Kimi Complex [35].

Cooling ages of 42-39 Ma obtained from K-Ar dating on micas indicate thermal evolution below 350-300 ºC of the lower unit, beneath the presumed detachment confining the Kesebir-Kardamos dome in Greece [29]. A single $^{40}Ar/^{39}Ar$ amphibole age of 45 Ma constrains cooling below 500 °C of the upper unit [13]. Supportively, $^{40}Ar/^{39}Ar$ data on micas from central and eastern Rhodope indicate Middle-Late Eocene cooling below 300-350 °C between 41-36 Ma [10, 13], followed by cooling to 150-300 ºC and exhumation at 23-12 Ma [10, 11]. Late- to post-tectonic plutons (e.g. Xanthi, Leptokaria, Simvolon) intruded the metamorphic units between 32-23 Ma [11, 22, 39]. The whole time span of volcanic activity in the eastern Rhodope region, including intrusion of subvolcanic bodies and dyke swarms, is bracketed between 37-21 Ma [25, 40-43] with the alkali basalts being emplaced in the Bulgarian side of the Kesebir-Kardamos and Biala reka-Kechros domes between 28-26 Ma [34].

Overall, the tectonometamorphic history of the eastern Rhodope took place during Mesozoic-Tertiary convergence and crustal thickening involving Late Paleozoic crustal material, which probably suffered high-pressure metamorphism at different times. It was followed by nearly isothermal decompression of rocks in extensional stages, regionally dominant since 38 Ma. Published ages on cooling history generally decrease southward, indicating the younging direction and downward crustal section progression of cooling and exhumation of distinct Rhodope units in the north Aegean domain.

3. Structural context of metamorphic domes

The large-scale tectonic pattern of the eastern Rhodope region is represented by gneiss domes, which have been recognized earlier under distinct names [44, 45]. The two principal structural domes are the Kesebir-Kardamos and the Biala reka-Kechros domes (Fig. 1), outlined by a pattern of amphibolite facies foliation in basement rocks. The dip of foliation wraps around the gneiss cores built by orthogneisses of the lower unit and flanked by structurally overlying upper unit meta-sedimentary and meta-igneous rocks.

The Kesebir river valley in Bulgaria exposes a NE-SW to NNE-SSW-trending Kesebir-Kardamos dome [46], which extends in northern Greece to the south (Fig. 2). It is cored by medium-pressure amphibolite facies migmatites and mainly orthogneisses of the lower tectonic unit, and mantled by a lithologically heterogeneous upper tectonic unit. Sillimanite-bearing migmatites indicate a late high-temperature overprint [47]. Both units in the northeastern side of the dome are juxtaposed against a major low-angle brittle fault – the Tokachka detachment, which is coupled with the underlying mylonites in normal dip-slip ductile shear zone that evolved in decreasing metamorphic grade from amphibolite to greenschist facies conditions. The detachment zone controlled sedimentation in the geometrically compatible supradetachment basin, filled with Maastrichtian-Palaeocene up to Early Eocene deposits of Krumovgrad Group [26], overlapped by Upper Eocene sediments which both sequences form the supracrustal sedimentary unit. A shear zone that bounds the southeastern side of the dome has oblique or horizontal lineations, and is interpreted as lower/upper unit decoupling zone that records

normal to dextral oblique ductile shear. The earliest deformation event in amphibolite facies is recognized in the upper unit, and resulted in a NW-SE trending stretching lineation comprising a top-to-the SSE ductile shear fabric. Subsequent deformation event caused pervasive mylonitization of the lower unit with NE-SW-oriented stretching lineation and top-to-the NNE ductile, then brittle shear. Localization of structures from ductile non-coaxial flow to semi-ductile and brittle deformation suggests a strain regime under constant direction from ductile to brittle field both in ductile mylonites and cataclasites in the detachment. This deformation led to strong thinning of the upper unit and extensional exhumation of the lower unit in the detachment footwall. The late stage deformation event accommodated brittle extension on high-angle normal and transtensional faults, and further contributed to sedimentation in detachment hanging-wall.

The Biala reka-Kechros dome is located about 20 km further east from the Kesebir-Kardamos dome (Fig. 1). Its exposure in southern Bulgaria continues into northern Greece. This more flat-lying and wide metamorphic dome exhibits coherent lithologic associations of both tectonic units, compared to the Kesebir-Kardamos dome, but is characterized by the presence of large ultrabasic slivers within the lower unit and poorly developed migmatites in the metamorphic sequence (Fig. 3). Similarly, the two main tectonic units are separated by brittle tectonic contact known as Pelevun thrust [44] at its northern tip. Our observations at the contact allowed an interpretation as detachment or décollement surface of wide regional extent. The two tectonic units are separated by the Kechros detachment that bounds the dome in Greece [29]. Geometrically and kinematically, the Biala reka-Kechros dome differs from the previous dome showing direction of tectonic transport towards SSW, which has been related either to syn-metamorphic thrusting [2] or an extensional faulting [29].

Our field and microscopic observations on shear structures and kinematics in Pelevun-Rosino area of the Biala reka-Kechros dome indicates a top-to-the SSW-directed shear in amphibolite facies, associated with N-S to NE-SW oriented stretching lineation in the basement gneisses (Fig. 3, 4a). In addition, the SSW-directed shearing evolved from amphibolite to greenschist facies conditions as recorded by mineral assemblages in the shear zone mylonites underlying the brittle detachment contact of both main units. They proceed to semi-ductile and brittle conditions in cataclastic zone, which defines the detachment itself (Fig. 4b). The peak amphibolite-facies mineral assemblage garnet-biotite-muscovite-staurolite at the vicinity of detachment is altered and contains chlorite after biotite and within strain shadows around garnet porphyroblasts, and secondary white mica crystallized along shear bands. The evolution of the shear zone mylonites is characterized by localization of ductile structures and change from ductile to semi-ductile deformation toward lower amphibolite facies conditions, with little or no greenschist retrogression. These deformation/crystallization relationships are supported further east below the corresponding detachment or décollement contact of both units under the low-grade Mesozoic schists [48], yet with consistently top-to-the SSW sense of shear (Fig. 3, 4c). However, the shear sense variation with respect to bulk south-directed shear, indicating opposite top-to-the NE tectonic transport (Fig. 4d), is observed mainly in the hanging wall upper unit. Here, the variation can be attributed to locally disturbed ductile flow pattern in enclosing rocks associated with emplacement of the Rosino granite, although this pattern may reflect NNE-directed tectonic displacement linked to complex kinematics and partitioned strain at the highest structural levels of the nappe system, as it has been suggested for the Central Rhodope [20] and the Serbo-Macedonian zone [4], possibly also related with extension. Alternatively, the shear sense variation may account for layer parallel extension during the detachment faulting.

Scarce magmatic bodies are spatially associated with or exposed adjacent to the metamorphic domes, which become more pronounced in volcanic centers further north, where the sedimentary basin widens. Several latitic and rhyolitic dykes have been established in the axial zone of the Kesebir-Kardamos dome, in addition to other relatively large and compositionally similar volcanic bodies at the flanks (Fig. 2). Numerous rhyolitic dykes of predominantly NNW-SSE strike intruded in the metamorphic rocks of the northern part of the Biala reka-Kechros dome followed by absarokite subvolcanic bodies (Fig. 3). The latest intra-plate basalts were emplaced along NW-SE, N-S and NE-SW striking faults within an E-W oriented area of both the Bila reka-Kechros and Kesebir-Kardamos domes [16, 34].

4. Ore deposits and mineralization

A newly discovered group of sedimentary-hosted epithermal Au deposits occurs spatially associated with the metamorphic domes. Two of these deposits, Ada Tepe and Rosino, have been studied in more detail [17, 49]. The Ada Tepe deposit is located in the supradetachment sedimentary sequence of Krumovgrad Group [26], overlying the northeastern closure of the Kesebir-Kardamos dome (Fig. 2). The contact between poorly consolidated strata and underlying metamorphic rocks is the detachment fault itself, separating a thin excised slice of the upper unit from the lower unit orthogneisses underneath. The hanging-wall suite is built up of blocks, breccias, breccia-conglomerates and sandstones. The provenance of clastic material is mainly from the gneisses, amphibolites, and marbles of the upper unit of the underlying metamorphic sequence.

The Rosino deposit is situated on the western faulted margin of an E-W- to NW-SE- elongated half-graben within the upper plate of detachment system in the center of the Biala reka-Kechros dome (Fig. 3). The older sediments (assumed belonging to the Krumovgrad Group) are exposed in the western and northeastern part of the half-graben. It consists of coarse breccias, breccia-conglomerates and sandstones with clastic material derived from low-grade Mesozoic rocks and high-grade metamorphic basement. Upper Eocene sediments

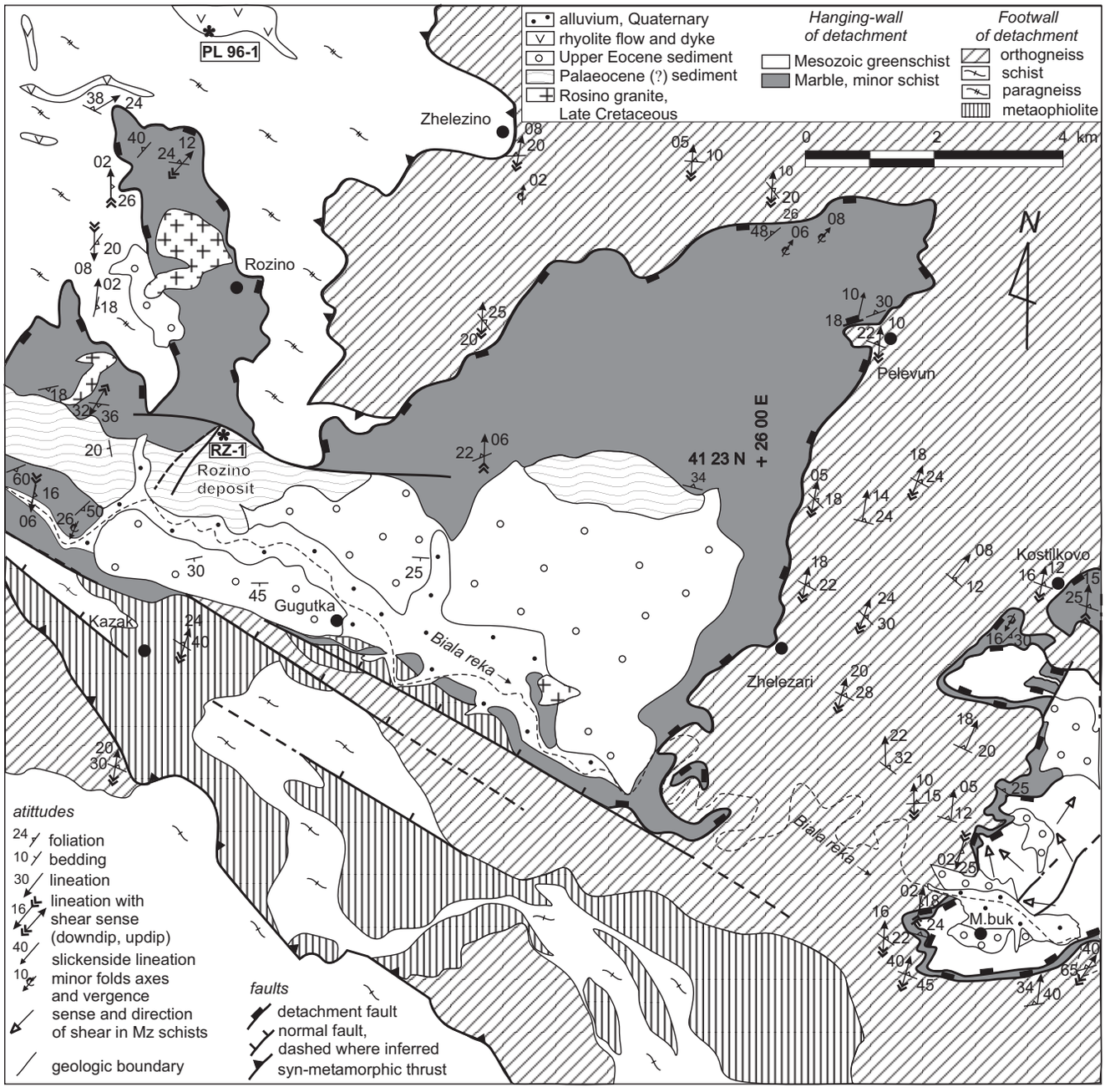

Figure 3: Simplified geological map of the Pelevun-Rozino area in the Biala reka-Kechros dome (by use the data from [48, 59, 60]) with own data of the kinematic direction in the rock units. Location of samples with $^{40}Ar/^{39}Ar$ analyses is indicated. See also table II.

occupy the central part of the half-graben, overlying the coarse clastic sediments. This sequence consists of sandstones, conglomerates, siltstones, mudstones and lignitic marls. The south to west-southwest and northeast dip of sedimentary bedding is generally consistent with the bulk southward tilt on the down-throw side of the half-graben bounding fault, suggesting that sedimentation is synchronous with normal faulting in the hanging wall of the detachment.

Gold mineralization at Ada Tepe and Rosino can be classified as low sulphidation epithermal type. Ada Tepe deposit [49] is characterized by silica-adularia-pyrite±sericite alteration, followed by silicification and gold mineralization, and late carbonates. Sites of mineralization include tabular ore body just above the detachment and open space-filling ores along predominantly east-west oriented high-angle faults in the hanging wall that sole into the detachment. Gold mineralization is typically electrum (Au/Ag~3) deposited from colloidal silica and gold particles.

Gold mineralization in the Rosino deposit is generally associated with a N-NE- trending normal fault bounding the half-graben. The host sedimentary rocks are strongly mylonitized, overprinted by a low-sulfidation alteration of adularia, quartz, sericite and pyrite. Highest-grade gold intervals are associated

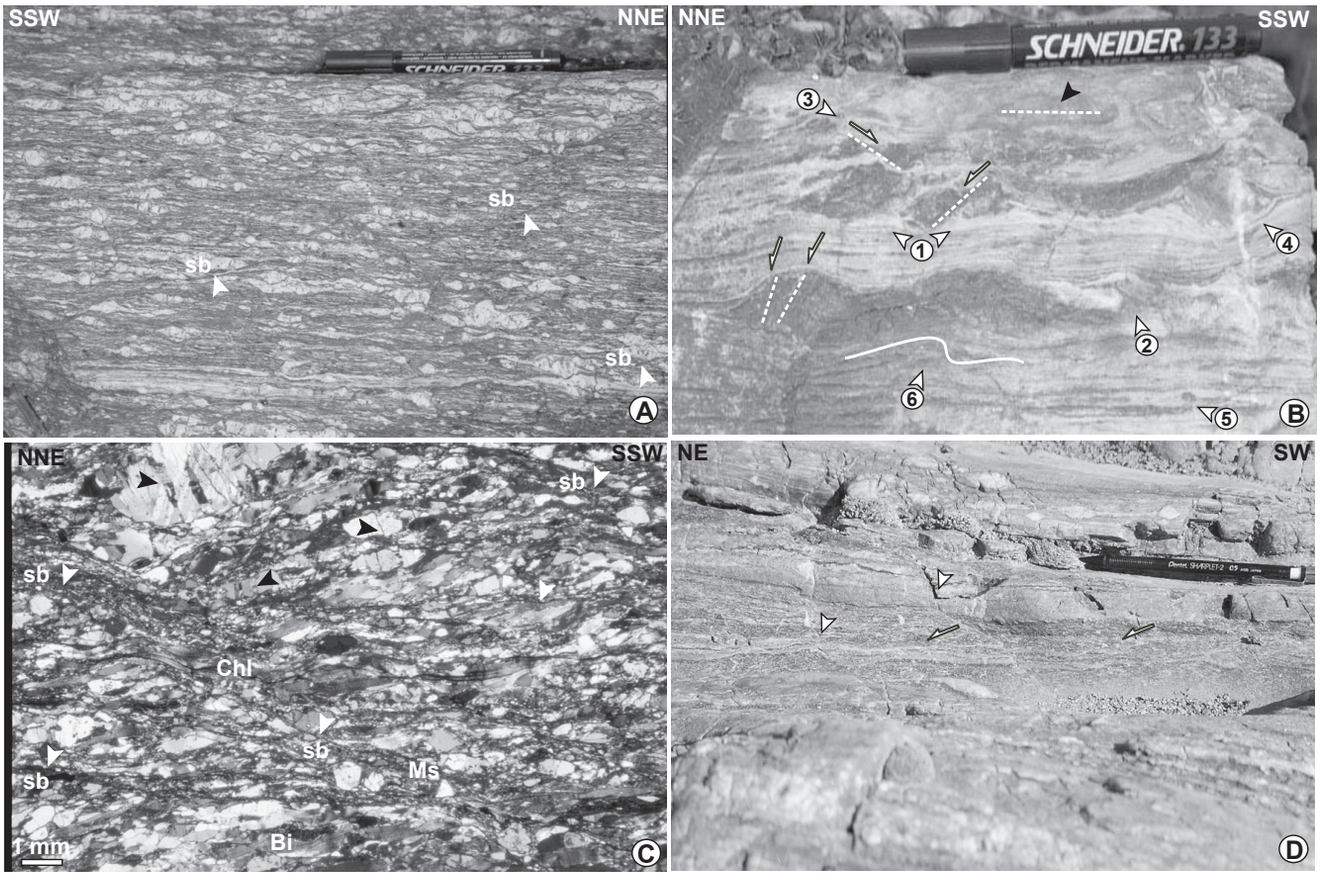

Figure 4: Field and microphotographs of structures and kinematics in the central Biala-reka-Kechros dome.
(a) Augen orthogneiss from the lower unit with shear structures sb = shear bands (white arrows), indicating sinistral shear (top-to SSW).
(b) Asymmetrically boudinaged calc-silicate layers in marbles. The deflection of marker horizon (1), asymmetric necking of foliation (2), normal-drag shear band with extensional offset (3), σ-type (4) and δ-type (5) clasts, and fold (6) all suggest dextral shear (top-to-SSW). The top surface (with marker) represents cataclastic plane of the detachment. Note elongated boudins surrounded by dark seams (black arrow), whose axes parallels striation lineation.
(c) Shear bands (sb) in mylonitic gneiss (white arrows) containing chlorite after biotite in the shear zone from below detachment surface, dextral shear (top-to SSW). Note ductile behavior of quartz and micas, relative to brittle fracturing of feldspars (black arrows), suggesting semi-ductile strain regime.
(d) Two-mica gneiss from the upper unit with structures (half arrows), indicating sinistral shear (top-to NE). Late microfaults (white arrows) offset quartzo-feldspatic layering.

with small amount of sulfide deposited at the margins of thin quartz-adularia-carbonate veinlets cutting the mylonites.

5. $^{40}Ar/^{39}Ar$ geochronology

5.1 Analytical techniques

In order to constrain the cooling/exhumation history of the metamorphic domes, $^{40}Ar/^{39}Ar$ laser-probe experiments on biotite and muscovite from metamorphic rocks were conducted in this study. We combined new $^{40}Ar/^{39}Ar$ laser-probe data on micas with results on adularia from the hydrothermally altered rocks, and sanidine and biotite from volcanic rocks of a companion paper [17], along with published data on amphibole and muscovite [10, 13] as to refine the timing of events in both domes, and compare the temporal evolution of tectonic, ore-forming and magmatic processes.

The $^{40}Ar/^{39}Ar$ laser-probe experiments were performed on a biotite and a muscovite separates from gneiss samples in the lower plate of the Kesebir-Kardamos dome. Biotite and muscovite were separated from 100-250 μm sieve fraction using standard magnetic and density methods. A final handpicking for the purity of the mineral concentrates was carried out under a binocular microscope. The small fraction (e.g.5 mg) of each mineral separate were irradiated with fast neutron in the CLICIT facility of TRIGA reactor at Oregon State University along with 27.92 Ma sanidine from the Taylor Creek rhyolite (TCRs) [50] as the neutron fluence monitor, with an intercalibrated age of 28.34 Ma [51], with ± 0.5% 1σ. The samples were analyzed by incremental heating experiment on 2-3 mg multi-crystal aliquots, using a defocused CO_2 laser beam. The isotopic composition of the argon gas in each heating step was measured by noble gas mass spectrometer MAP 215-50 in the Rare Gas Geochronology Laboratory at the University of Wisconsin-Madison, U.S.A. All data and

Table I

Incremental heating experiments

36 Ar(a)	37 Ar	38 Ar	39 Ar(K)	40 Ar(r)	Age + 2σ	40 Ar(%)	39Ar(K)(%)
Sample H-706 muscovite (irradiation value J=0.002976)							
0,00000	0,00000	0,00001	0,00250	0,01187	25.27± 136.47	99,90	0,04
0,00279	0,00168	0,00015	0,24116	1,70050	37.47± 1.86	67,35	3,75
0,00180	0,01181	0,00033	0,65028	4,67472	38.19± 0.69	89,71	10,10
0,00154	0,02920	0,00056	1,30920	9,31474	37.80± 0.35	95,29	20,33
0,00117	0,01770	0,00044	1,28480	9,21613	38.11± 0.35	96,32	19,96
0,00096	0,00915	0,00054	1,14844	8,34471	38.60± 0.39	96,64	17,84
0,00008	0,00294	0,00044	0,80086	5,90493	39.16± 0.56	99,53	12,44
0,00033	0,00301	0,00013	0,35568	2,61266	39.01± 1.26	96,36	5,52
0,00033	0,00378	0,00022	0,64545	4,69190	38.61± 0.69	97,91	10,03
Results		40(r)/39K	±2σ	Age (Ma)	2σ		
Weighted plateau		7.1775	±0.0530	38.13	±0.36		
Total fusion		7.2180	±0.0389	38.34	±0.31		
Sample H-6 biotite (irradiation value J=0.002976)							
0,00008	0,00025	0,00004	0,00250	0,00902	19.27± 12.32	27,58	0,07
0,00271	0,01246	0,00560	0,39919	2,69081	35.83± 0.17	77,05	11,11
0,00068	0,00611	0,00960	0,69053	4,91896	37.85± 0.14	96,03	19,22
0,00045	0,01232	0,00790	0,65010	4,60775	37.66± 0.13	97,16	18,10
0,00029	0,00529	0,00617	0,47901	3,39959	37.71± 0.16	97,45	13,33
0,00030	0,00378	0,00778	0,58544	4,15267	37.69± 0.31	97,83	16,30
0,00019	0,00810	0,00525	0,38650	2,76814	38.05± 0.20	97,98	10,76
0,00012	0,00384	0,00498	0,39891	2,84570	37.90± 0.09	98,70	11,10
Results		40(r)/39K	±2σ	Age (Ma)	2σ		
Weighted plateau		7.1020	±0.0176	37.73	±0.25		
Total fusion		7.0689	±0.0137	37.56	±0.24		

Table I: $^{40}Ar/^{39}Ar$ analytical data for incremental heating experiments on muscovite and biotite from the Kesebir-Kardamos dome in the Eastern Rhodope, Bulgaria.

uncertainties are presented with a 2σ analytical error. Analytical procedure, blank corrections and estimation of uncertainties are described in detail by Singer and Brown [52].

5.2 Samples used for the 40Ar/39Ar analysis

Sample locations of the analyzed muscovite and biotite mineral separates are shown on geological map of Fig. 2, and are described below as follows.

Sample H-6 represents an augen gneiss mylonite taken from the shear zone in the footwall of the detachment in the northern flank of the Kesebir-Kardamos dome (Fig. 2, 5a). Mineral assemblage consists of quartz, plagioclase, K-feldspar, biotite ± muscovite and garnet. The mica flakes and asymmetric K-feldspar porphyroclasts indicate top-to-the NNE tectonic transport, associated with lower temperature condition of deformation in the sample relative to the high-temperature deformation fabrics in migmatites (> 600 °C) structurally below, and relatively higher than the fabrics in retrogressed schists on the structural top of the shear zone. No secondary mica generations or alteration products are observed in this sample. Therefore, the metamorphic temperatures, inferred from deformation-crystallization relationships and quartz c-axis fabrics (<500 °C) in nearby localities, as well as appropriate structural position just below cataclastic zone that defines the detachment, are all in favor to date micas (biotite in the case) by applying $^{40}Ar/^{39}Ar$ technique to obtain the closure of argon isotope system after amphibolite facies metamorphism.

Sample H-706 is taken from the muscovite gneisses that can be continuously traced along the mylonitic contact on southeastern flank of the Kesebir-Kardamos dome (Fig. 2, 5b). Analyzed white mica is represented by muscovite porphyroclasts that define a foliation and weak shear fabric, indicating top-to-the NE tectonic transport. A single white mica generation is identified in the metamorphic assemblage of the thin section. Other mineral phases in the metamorphic assemblage includes, in decreasing modal proportions, quartz, plagioclase and garnet ± staurolite.

5.3. Results and interpretation

The analytical results of incremental heating experiments are listed in table I and are presented as age spectra in figure 6, all with a corresponding 2σ analytical error.

Incremental heating experiments on a biotite and muscovite separates from the samples of mica-bearing metamorphic

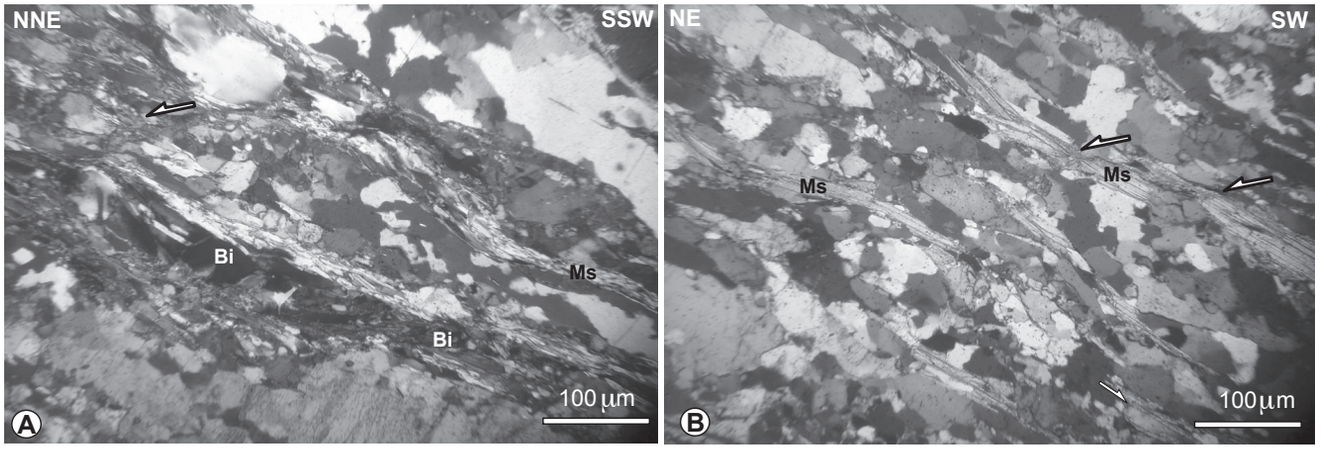

Figure 5: Samples of metamorphic rocks used for the $^{40}Ar/^{39}Ar$ geochronology.
(a) Microphotograph of mica fabric in augen orthogneiss (sample H-6) from shear zone below the detachment.
b) Microphotograph of muscovite gneiss (sample H-706) on southeastern flank of the Kesebir-Kardamos dome. Shear structures are indicated (half arrows).

rocks resulted in a well-defined flat age spectra (Fig. 6). They indicate the lack of multiple mica populations presented in the analyzed samples as opposed to staircase pattern characteristic of outgasing mixed populations, and thus fit well to the macro-and microfabric observations, and suggest absence of rejuvenation or reheating of the argon isotopic system. The results of the $^{40}Ar/^{39}Ar$ incremental heating experiments on muscovite in gneiss (sample H-706) reveal a plateau age of 38.13 ± 0.36 Ma (Fig. 6a, table I) that is indistinguishable from the total fusion age (38.34 ± 0.31 Ma). The incremental heating experiments on biotite from augen orthogneiss (sample H-6) results in an age of 37.73 ± 0.25 Ma of weighted plateau from a concordant six-steps, yet similar to the total fusion age (37.56 ± 0.24 Ma) (Fig. 6b, table I). Metamorphic crystallization of mineral assemblages in both gneiss samples indicate that analyzed micas have crystallized at temperatures above relevant closure temperature range for argon isotope system in micas (350 ± 30°C and 300 ± 20°C in white mica and biotite [53, 54], respectively). We interpret the new ages from metamorphic rocks as dating the cooling of the lower unit rocks below 350-300 °C related to the tectonic emplacement of the dome, when deformation proceeded from ductile to semi-ductile conditions.

Localities of published data from other metamorphic rocks (Fig. 1), and hydrothermally altered rocks and volcanic rocks used in this paper are presented in figure 2 and figure 3. Ages and short descriptions of the samples are given in table II.

Adularia from alteration zone at Ada Tepe deposit (sample AT01-2) formed at 34.99 ± 0.23 Ma, slightly younger than the adularia age of 36.46 ± 0.26 Ma from the Rosino deposit (sample Rz-1) (table II). The crystallization ages of adularia from hydrothermally altered rocks are regarded as dating the late stage brittle deformation associated with high-angle normal faults in the hanging-wall of the detachments, as adularia typically crystallized in altered halo around ore-filled fractures and the fractures themselves.

Sanidine from rhyolite dyke (sample AT01-17) in the core of the Kesebir-Kardamos dome yielded an age of 31.82 ± 0.20 Ma, whereas biotite from a rhyolite flow (sample PL96-1) in the Biala reka-Kechros dome reveals an age of 32.88 ± 0.23 Ma (table II). The ages of the magmatic rocks are younger than alteration and coincide with the timing of main phase volcanic activity as recorded elsewhere in the eastern Rhodope [40-43].

In the Biala-reka-Kechros dome, the $^{40}Ar/^{39}Ar$ determinations of amphibole in retrograded eclogite from the upper unit in Bulgaria yield 45 ± 2 Ma, whereas muscovite in the schists gives an age of 39 ±1 Ma [13]. In Greece, muscovite ages of the lower unit that is exposed in the southern part of the dome cluster in the time interval between 41 and 36 Ma [10] (see Fig. 1).

In summary, the new $^{40}Ar/^{39}Ar$ age determinations of micas from metamorphic rocks, along with those from the hydrothermal alteration and volcanic rocks defines an approximately 6-7 Ma lasting time interval, which brackets cooling of the metamorphic basement, ore-forming and magmatic processes. Ore formation at 36.5-35 Ma temporarily overlaps with the regional cooling and exhumation of the basement between 41-36 Ma. Volcanic dykes post-date the main phase of cooling/exhumation of the basement and mineralization.

6. Discussion

6.1. Thermotectonic evolution and interaction between distinct processes in the Eastern Rhodope

The new $^{40}Ar/^{39}Ar$ ages on muscovite and biotite of metamorphic rocks in this study, along with those from magmatic and ore-forming rocks and existing $^{40}Ar/^{39}Ar$ published data, allow to identify the thermotectonic history of rock units in the detachment fault systems.

The analyzed mica-bearing samples of metamorphic rocks provide age constraints on cooling history of the footwall across the Kesebir-Kardamos dome at the vicinity of the

Table II

Sample	Mineral	Description	Location	Total fusion age (Ma) + 2σ	Weighted plateau age (Ma) + 2σ	Reference
AT01-2	Adularia	Low-sulfidation alteration	Ada Tepe deposit Kesebir-Kardamos dome northeastern closure	35.05 ± 0.23	34.99 ± 0.23	Marchev et al. (in press)
AT01-17	Sanidine	Rhyolite dyke	Kesebir-Kardamos dome core zone	31.88 ± 0.20	31.82 ± 0.20	Marchev et al. (in press)
Rz-1	Adularia	Low-sulfidation alteration	Rosino deposit Biala reka-Kechros dome	36.45 ± 0.25	36.46 ± 0.26	Marchev et al. (in press)
PL 96-1	Biotite	Rhyolite body	Biala reka-Kechros dome northern closure	32.94 ± 0.26	32.88 ± 0.23	Marchev et al. (in press)
	Amphibole	Eclogite	Biala reka-Kechros dome northern closure	45.00 ± 2.00		Mukasa et al. (2003)
	Muscovite	Metapelite	Biala reka-Kechros dome northern closure	39.00 ± 1.00		Mukasa et al. (2003)
437	White mica clast	Granite mylonite	Biala reka-Kechros dome southern part	39.30 ± 6.90	39.30 ± 5.40	Lips et al. (2000)
437	White mica clast	Granite mylonite	Biala reka-Kechros dome southern part	spot fusion age	37.60 ± 1.09	Lips et al. (2000)
437	White mica foliation-forming	Granite mylonite	Biala reka-Kechros dome southern part	35.90 ± 6.70	35.30 ± 4.40	Lips et al. (2000)
438	White mica clast	Augengneiss	Biala reka-Kechros dome southern part	43.00 ± 4.00	42.40 ± 2.30	Lips et al. (2000)
438	White mica clast	Augengneiss	Biala reka-Kechros dome southern part	spot fusion age	41.09 ± 1.20	Lips et al. (2000)
438	White mica foliation-forming	Granite mylonite	Biala reka-Kechros dome southern part	36.10 ± 5.80	36.20 ± 4.30	Lips et al. (2000)
438	White mica foliation-forming	Granite mylonite	Biala reka-Kechros dome southern part	spot fusion age	36.00 ± 0.70	Lips et al. (2000)

Table II: Summary of available $^{40}Ar/^{39}Ar$ ages for the metamorphic, and volcanic rocks and alteration in the Kessebir-Kardamos and the Biala reka-Kechros domes in the Eastern Rhodope of south Bulgaria and northern Greece.

lower orthogneiss unit/upper variegated unit contact. The 38-37 Ma mica ages constrains cessation of ductile activity on shear zones and subsequent continuation at semi-brittle conditions, whose onset was initiated earlier as deduced from amphibolite facies metamorphic assemblages in the shear zones, as well as in the core-zone orthogneisses. Minimal age differences in both flanks are attributed as to reflecting $^{40}Ar/^{39}Ar$ cooling age of previously developed mica fabric in high-grade rocks below nominal closure temperatures of argon isotope system in micas. Therefore, the tectonic displacement on these ductile shear zones most likely ceased after the time indicated by the $^{40}Ar/^{39}Ar$ plateau ages (i.e. between 38-37 Ma), and further continued to operate under semi-ductile to brittle low-temperature conditions.

The ages of 36.5-35 Ma indicate crystallization of adularia in alteration zones at Rosino and Ada Tepe deposits on detachment hanging-wall units in the Biala reka-Kechros and Kesebir-Kardamos domes, respectively, which have been developed at brittle crustal conditions during or subsequent to cooling of the basement rocks, when temperatures dropped to below 200°-150 °C (average closure temperature range of argon in alkali feldspars [54]). This temperature range fully coincides to T < 200 °C derived from palaeotemperature analysis of alteration at Ada Tepe deposit [17]. We argue that the later ages temporarily

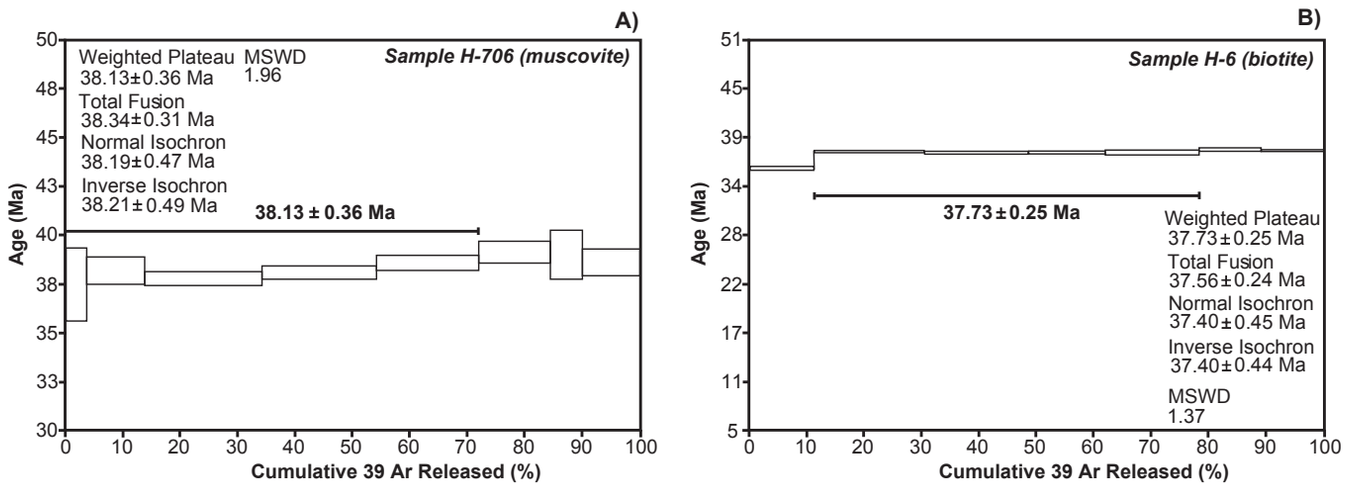

Figure 6: $^{40}Ar/^{39}Ar$ age spectra of muscovite and biotite from the Kesebir-Kardamos dome, Eastern Rhodope. Experimental temperatures increase from left to right. Plateau ages are indicated with increments used for calculation. Total fusion age, normal and inverse isochrons are also shown.

correspond to the time interval at which the total metamorphic sequence was at very shallow crustal levels in the brittle field, affected mainly by brittle faulting in both footwall and predominantly hanging-wall units of the detachment system.

Muscovite and biotite ages in this study together with the age of adularia provide temperature window from as high as 350 °C to as low as 150 °C between 38-35 Ma, possibly indicating rapid cooling of the footwall and hanging-wall units in detachment system of the Kesebir-Kardamos dome. Similarly, if we take into account $^{40}Ar/^{39}Ar$ amphibole and muscovite ages [13] in the Biala reka-Kechros dome, assuming that the muscovite sample belongs to the upper plate rocks, than cooling of the upper unit from as high as 500 °C to as low as 350 °C occurred between 45-39 Ma, which implies a cooling rate between 17 and 50 °C Myr^{-1} after amphibolite facies metamorphism. Following the ca. 36-35 Ma entirely brittle event, subsequent magmatic activity is recorded in both domes within the time interval of 33-32 Ma and 28-26 Ma, as indicated by $^{40}Ar/^{39}Ar$ and K/Ar crystallization ages of rhyolite and intraplate basaltic dykes, respectively.

Our geochronologic results show that cooling and exhumation of lower unit from the Kesebir-Kardamos dome in the footwall of detachment have occurred between 38 and 37 Ma. Regionally, the initiation of magmatic activity in Late Eocene (Priabonian) coincides with cooling and extensional exhumation of metamorphic lower unit in the footwall of the detachments around ca. 38-37 Ma. As extension continued to operate on normal faults under brittle conditions at shallow crustal levels, hydrothermal alteration took place in both epithermal deposits in the hanging walls around 36-35 Ma. Therefore, the $^{40}Ar/^{39}Ar$ ages testified for the temporal interference between extensional tectonics, ore-forming mineralization and magmatic activity. All these processes interact during the late orogenic extensional collapse in the Eastern Rhodope showing regionally overlapping Late Eocene ages. In addition, the $^{40}Ar/^{39}Ar$ results suggest that epithermal mineralizations spatially associated to metamorphic domes are related to permeable fault zones through activation of low-angle detachments rather than linked to magmatic activity [49].

6.2. Inferences on timing and mode of crustal extension in the Eastern Rhodope

The onset of crustal extension in the Eastern Rhodope region is indicated from the stratigraphic information of sedimentary sequences in the hanging-wall of detachment faults. The initiation of extension at Palaeocene-Eocene boundary is documented by Maastrichtian-Palaeocene sediments of Krumovgrad Group [26], whose upper stratigraphic levels reaches Lower Eocene (Ypresian), which stratigraphic age is also corroborated by the Lutetian sediments unconformably overlaying the metamorphic sequence in northern Greece [29, 55]. This suggests that by Early Eocene time (ca. 53-46) the upper unit have been exposed at the surface through activation of extensional detachments. Subsequently, as extension progressed, exhumation of the lower unit in the footwalls of detachments and widespread cooling of mid-crustal rocks have occurred between 41-36 Ma as indicated by common white mica and biotite $^{40}Ar/^{39}Ar$ ages derived from this study and published geochronologic data [10, 13].

The metamorphic domes in the Eastern Rhodope display many features characteristic for metamorphic core complexes such as detachment faults underlain by shear zones that record evolution from ductile to brittle deformation conditions. They are similar to the metamorphic domes in many orogens, whose origin is attributed to different processes such as diapirism, crustal shortening and extension [56–58]. Each of these models predicts variety on the nature of structural boundary between gneissic core and surrounding mantle rocks, as well as on the spatial distribution and variation of cooling history that would be expected within the gneiss dome. The regional constraints on tectonostratigraphy, structural and metamorphic history, connected with available geochronologic data, unequivocally support an extensional origin of the metamorphic domes in the eastern Rhodope region.

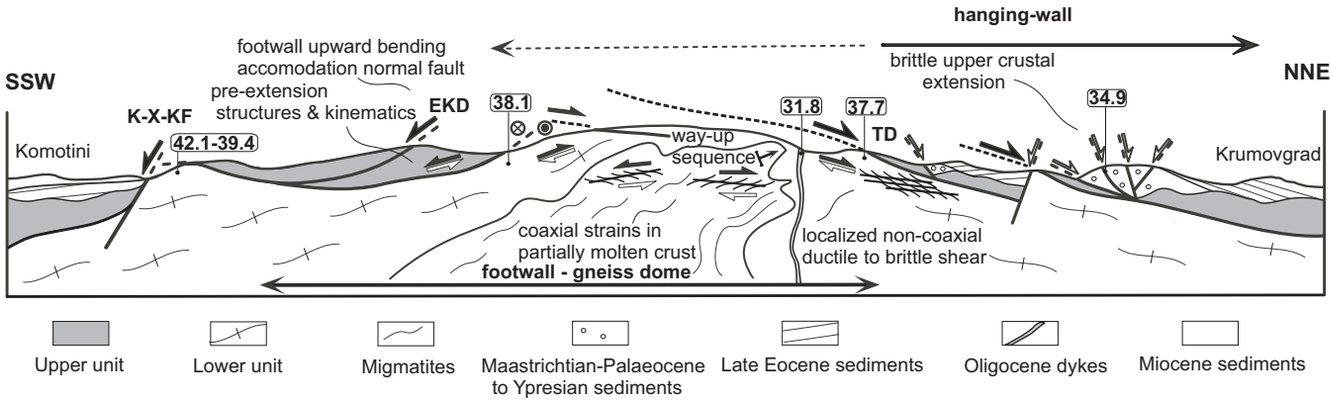

Figure 7: Interpretative cross-section of the Kesebir-Kardamos dome (not to scale), depicting structural geometry and kinematics, and showing ages and elements of the extensional detachment system along NE-SW traverse from Krumovgrad to Komotini in southern Bulgaria and northern Greece. See also Fig. 1 for the location.

The integration of the results from structural and geochronologic studies at latitude of the Kesebir-Kardamos dome is presented in synthetic cross-section through south Bulgaria and northern Greece (Fig. 7). The hanging-wall upper unit was exhumed earlier at least as late as Early Eocene (ca. ~ 46 Ma) as discussed above. The spatial distribution of ages within the lower unit suggests a temporal evolution of cooling and exhumation history from structurally lower to structurally higher levels of metamorphic sequence. Incorporation of our $^{40}Ar/^{39}Ar$ mica ages with published K/Ar results in Greece [29] defines variations of cooling history on both flanks across the dome. The data show a gradual decrease in mica cooling ages up structural section all along southern flank from 42-39 Ma in Greece to 38 Ma in Bulgaria, and their northward younging down structural section on the northern flank to 37 Ma, and finally to 35 Ma associated with younger north-dipping faults in the hanging-wall just above the detachment surface. This implies that the dome cooled asymmetrically as a result of southward exhumation of the footwall, consistent with the northward decrease of cooling ages towards the detachment. Consequently, the lower unit rocks were "captured" in the shear zone beneath the detachment and "transported" in the footwall, and the exhumed portion of the metamorphic sequence was gradually "closed" for argon isotope system in micas as ongoing deformation proceeded from the ductile to the brittle field. This spatial distribution of ages sketches an asymmetric mode of crustal extension at latitude of the Kesebir-Kardamos dome, to which regional-scale variation in the sense of tectonic displacement could be added. We suggest with respect to the regional tectonic pattern, that the Avren fault (see Fig. 1) acted as left-lateral/normal transfer fault zone during Late Eocene, linking both domes as different domains in the Eastern Rhodope extensional system, yet with consistent but opposed sense of tectonic displacement and variation in sense and direction of shear, while deep syn-metamorphic thrusting was still active at depth. This feature is evidenced by the available geochronologic data in both domes, that share similar cooling ages, the preserved kinematics of nappe stacking towards SSW within the lower unit in the Biala reka-Kechros dome, which is totally erased by migmatization and pervasive extensional shearing in the lower unit of the Kesebir-Kardamos dome.

7. Conclusions

The $^{40}Ar/^{39}Ar$ dating on micas from metamorphic rocks in this study, combined with similar data of magmatic and hydrothermally altered rocks, allows temporal constraints on timing of events involved during late-orogenic extension in the eastern Rhodope region. Several critical points on the establishment of temporal sequence of events are sketched as follows.

1. Following an earlier exhumation of the upper unit as lately ca. 53-46 Ma, the lower unit of the metamorphic basement that typified domes in the footwall of detachments, had cooled below 350°-300 °C between 38-37 Ma. The latter ages further refine the cooling and exhumation history of metamorphic sequence, suggesting that an episode of regional cooling of the lower unit occurred between 42-36 Ma as indicated by similar white mica and biotite ages (this study and previous data).

2. Ore deposits formation in the time interval ca. 36.5-35 Ma in the hanging-wall of detachments associated with late stage brittle extension on high-angle faults was coeval to subsequent of cooling, extensional exhumation and final doming of the lower unit in their footwalls.

3. $^{40}Ar/^{39}Ar$ ages provide a thermotectonic window after amphibolite facies metamorphism of ductile then brittle deformation from as high as 350 °C to as low as 150 °C between 38-35 Ma. At latitude of the Kesebir-Kardamos dome they define an asymmetric cooling history and mode of crustal extension.

4. Following amphibolite facies metamorphism and emplacement of granitoids in the Late Cretaceous, cooling and exhumation of the metamorphic basement rocks occurred afterwards, which, in turn, was followed by epithermal mineralization and Late Eocene-Oligocene volcanism. The onset of volcanism in Priabonian temporarily coincides with the cooling of the metamorphic basement. The main phase

of volcanic activity in Early Oligocene between 33-32 Ma is well documented in both metamorphic domes. These new $^{40}Ar/^{39}Ar$ data suggests that all above tectonic, ore-forming and magmatic processes interfered during late-orogenic extension in the eastern Rhodope region.

Acknowledgments

This study was carried under the framework of SCOPES program and supported by ABCD-GEODE project on "*Evolution of Magmatism and Mineralization in the Eastern Rhodope Region with Relation to Extensional Tectonics*". $^{40}Ar/^{39}Ar$ analyses at UW-Madison were supported by US NSF grants EAR-0114055 and EAR-0337667 to Singer. Constructive reviews by Andor L.W. Lips and two anonymous referees on previous version of the manuscript have been appreciated and helped to improve the article. The authors greatly acknowledge editorial assistance of Prof. E. Bozkurt on this contribution to Special Thematic Issue of the journal.

References

[1] Schermer E.R., Geometry and kinematics of continental basement deformation during the Alpine orogeny, Mount Olympos region, Greece, J. Struct. Geol. 15 (1993) 571-591.

[2] Burg J-P., Ricou L-E., Ivanov Z., Godfriaux I., Dimov D., Klain L., Syn-metamorphic nappe complex in the Rhodope Massif. Structu re and kinematics, Terra Nova 8 (1996) 6-15.

[3] Dinter D.A., Late Cenozoic extension of the Alpine collisional orogen, northeastern Greece: Origin of the north Aegean basin, Geol. Soc. Am. Bull. 110 (1998) 1208-1230.

[4] Kilias A., Falalakis G., Mountrakis D., Cretaceous-Tertiary structures and kinematics of the Serbomacedonian metamorphic rocks and their relation to the exhumation of the Hellenic hinterland (Macedonia, Greece), Int. J. Earth Sci. 88 (1999) 513-531.

[5] Okay A. I., Satir M., Coeval plutonism and metamorphism in a latest Oligocene metamorphic core complex in Northwest Turkey, Geol. Mag. 137 (2000) 495-516.

[6] Lips A.L.W., Temporal constraints on the kinematics of the destabilization of an orogen: syn- to post-orogenic extensional collapse of the Northern Aegean region, PhD thesis, Utrecht University, Geologica Ultraectina 166, 1998, 224 p.

[7] Lips A.L.W., White S.H., Wijbrans J.R, $^{40}Ar/^{39}Ar$ laserprobe direct dating of discrete deformational events: a continuous record of early Alpine tectonics in the Pelagonian Zone, NW Aegean area, Greece, Tectonophysics 298 (1998) 133-153.

[8] Lips A.L.W., Wijbrans J.R, White S.H., New insights from $^{40}Ar/^{39}Ar$ laserprobe dating of white mica fabrics from the Pelion Massif, Pelagonian Zone, Internal Hellenides, Greece: implications for the timing of metamorphic episodes and tectonic events in the Aegean region, in: Durand, B., Jolivet, L., Horváth, F., Séranne, M. (Eds.), The Mediterranean Basins: Tertiary Extension within the Alpine Orogen, Geol. Soc. London Spec. Publ., 156, Blackwell, Oxford, 1999, pp. 457-474.

[9] Peycheva I., Quadt A.V., (1995) U-Pb zircon dating of metagranites from Byala Reka region in the east Rhodopes, Bulgaria, in: Papanikolaou, D. (Ed.) Proc. 15th Congr. Carpatho-Balkan Geol. Assoc., Geol. Soc. Greece Sp. Publ. 4/2, Athens, 1995, pp. 637-642.

[10] Lips A.L.W., White S.H., Wijbrans J.R., Middle-Late Alpine thermotectonic evolution of the southern Rhodope Massif, Greece, Geodin. Acta 13 (2000) 281-292.

[11] Dinter D.A., Macfarlane A.M., Hames W., Isachsen C., Bowring S., Royden L., U-Pb and $^{40}Ar/^{39}Ar$ geochronology of the Symvolon granodiorite: implications for the thermal and structural evolution of the Rhodope metamorphic core complex, northeastern Greece, Tectonics 14 (1995) 886-908.

[12] Wawrzenitz N., Krohe A., Exhumation and doming of the Thasos metamorphic core complex (S Rhodope, Greece): structural and geochronological constraints, Tectonophysics 285 (1998) 301-332.

[13] Mukasa, S.B., Haydoutov, I., Carrigan, C.W., Kolcheva, K., Thermobarometry and $^{40}Ar/^{39}Ar$ ages of eclogitic and gneissic rocks in the Sredna Gora and Rhodope terranes of Bulgaria, J. Czech Geol. Soc. 48 (2003) 94-95.

[14] Dewey J., Extensional collapse of orogens, Tectonics 7 (1988) 1123-1139.

[15] Liu, M. Cenozoic extension and magmatism in the North American Cordillera: the role of gravitational collapse, Tectonophysics 342 (2001) 407-433.

[16] Marchev, P., Raicheva, R., Downes, H., Vaselli, O., Chiaradia, M., R. Moritz., Compositional diversity of Eocene-Oligocene basaltic magmatism in the Eastern Rhodopes, SE Bulgaria: implications for its genesis and relations to extensional tectonics, (Tectonophysics, in press)

[17] Marchev, P., Singer, B.S., Jelev D., Hasson S., Moritz, R., Bonev N., The Ada Tepe deposit: a sediment-hosted, detachment fault-controlled, low-sulfidation gold deposit in the Eastern Rhodopes, SE Bulgaria, (Schweiz. Mineral. Petrogr. Mitt., in press).

[18] Robertson A.H.F., Dixon J.E., Brown S., Collins A., Morris A., Pickett E., Sharp I., Ustaömer T., Alternative tectonic models for the Late Palaeozoic-Early Tertiary development of Tethys in the Eastern Mediterranean region, in: Morris A., Tarling D.H. (Eds.), Paleomagnetism and Tectonics of the Mediterranean Region, Geol. Soc. London Sp. Publ. 105, Blackwell, Oxford, 1996, pp. 239-263.

[19] Stampfli, G.M, Borel, J.D., A plate tectonic model for the Paleozoic and Mesozoic constrained by dynamic plate boundaries and restored synthetic oceanic isochrones, Earth Planet. Sci. Lett. 196 (2002) 17-33.

[20] Ricou L-E., Burg J-P., Godfriaux I., Ivanov Z., Rhodope and Vardar: the metamorphic and the olistostromic paired belts related to the Cretaceous subduction under Europe, Geodin. Acta 11 (1998) 285-309.

[21] Soldatos T., Christofides G., Rb-Sr geochronology and origin of the Elatia Pluton, Central Rhodope, North Greece, Geol. Balc. 16 (1986) 15-23.

[22] Jones C. E., Tarney J., Baker J.H., Gerouki F., Tertiary granitoids of Rhodope, northern Greece: magmatism related to extensional collapse of the Hellenic Orogen?, Tectonophysics 210 (1992) 295-314.

[23] Ovtcharova M., Quadt A.V., Heinrich C.A., Frank M., Kaiser-Rohrmeier M., Triggering of hydrothermal ore mineralization in the Central Rhodopean Core Complex (Bulgaria) – Insights from isotope and geochronological studies on Tertiary magmatism and migmatization, in: Eliopoulos D.G. *et al*. (Eds.), Mineral Exploration and Sustainable Development 1, 2003, Millpress, Rotterdam, pp. 367-370.

[24] Harkovska A., Yanev Y., Marchev P., General features of the Paleogene orogenic magmatism in Bulgaria, Geol. Balc. 19 (1989) 37-72.

[25] Yanev Y., Innocenti F., Manetti P., Serri G., Upper-Eocene-Oligocene collision-related volcanism in eastern Rhodopes (Bulgaria) – Western Thrace (Greece): petrogenetic affinity and geodynamic significance, Acta Vulcanologica 10 (1998) 279-291.

[26] Goranov A., Atanasov G., Lithostratigraphy and formation conditions of Maastrichtian-Palaeocene deposits in Krumovgrad District, Geol. Balc. 22 (1992) 71-82.

[27] Boyanov I., Goranov A., Late Alpine (Palaeogene) superimposed depressions in parts of Southeast Bulgaria, Geol. Balc. 31 (2001) 3-36.

[28] Mposkos E., Krohe A., Petrological and structural evolution of continental high-pressure (HP) metamorphic rocks in the Alpine Rhodope Domain, in: Panaydes I., Xenophontos C., Malpas J. (Eds.), Proc. 3rd Int. Conf. Geology E. Mediterranean, Geol. Surv. Cyprus, Nicosia, 2000, pp. 221-232.

[29] Krohe A., Mposkos E., Multiple generations of extensional detachments in the Rhodope Mountains (northern Greece): evidence of episodic exhumation of high-pressure rocks, in: Blundell D.J., Neubauer F., von Quadt A. (Eds.), The Timing and Location of Major Ore Deposits in an Evolving Orogen, Geol. Soc. London Sp. Publ. 204, Blackwell, Oxford, 2002, pp.151-178.

[30] Mposkos E., Liati A., Metamorphic evolution of metapelites in the high-pressure terrane of the Rhodope zone, northern Greece, Can. Mineral. 31 (1993) 401-424.

[31] Mposkos E.D., Kostopoulos D.K., Diamond, former coesite and supersilicic garnet in metasedimentary rocks from the Greek Rhodope: a new ultrahigh-pressure metamorphic province established, Earth Planet. Sci. Lett. 192 (2001) 497-506.

[32] Marchev P., Rogers G., Conrey R., Quick J., Vaselli O., Raicheva R., Paleogene orogenic and alkaline basic magmas in the Rhodope zone: relationships, nature of magma sources, and role of crustal contamination, Acta Vulcanologica 10 (1998) 217-232.

[33] Yanev Y., Bardintzeff J-M., Petrology, volcanology and matallogeny of Palaeogene collision-related volcanism of the Eastern Rhodopes (Bulgaria), Terra Nova 9 (1997) 1-8.

[34] Marchev P., Vaselli O., Downes H., Pinarelli L., Ingram G., Rogers G., R. Raicheva R., Petrology and geochemistry of alkaline basalts and lamprophyres: implications for the chemical composition of the upper mantle beneath the Eastern Rhodopes (Bulgaria), Acta Vulcanologica 10 (1998) 233-242.

[35] Mposkos E., Wawrzenitz N., Metapegmatites and pegmatites braketing the time of HP-metamorphism in polymetamorphic rocks of the E. Rhodope, northern Greece: Petrological and geochronological constraints, in: Papanikolaou, D. (Ed.) Proc. 15th Congr. Carpatho-Balkan Geol. Assoc., Geol. Soc. Greece Sp. Publ. 4/2, Athens, 1995, pp. 602-608.

[36] Peycheva I., Ovtcharova M., Sarov S., Kostitsin J., Age and metamorphic evolution of metagranitoids from Kesebir reka region, Eastern Rhodopes–Rb-Sr isotope data, Carpathian-Balkan Geological Association, 16th Congress, Abstract, Vienna, 1998, p. 471.

[37] Wawrzenitz N., Mposkos E., First evidence for Lower Cretaceous HP/HT-metamorphism in the Eastern Rhodope, North Aegean Region, North-East Greece, Eur. J. Mineral. 9 (1997) 659-664.

[38] Liati A., Gebauer D., Wysoczanski R., U-Pb SHRIMP-dating of zircon domains from UHP garnet-rich mafic rocks and late pegmatoids in the Rhodope zone (N Greece); evidence for Early Cretaceous crystallization and Late Cretaceous metamorphism, Chem. Geol. 184 (2002) 281-299.

[39] Del Moro A., Innocenti F., Kyriakopoulos K., Manetti P., Papadopoulos P., Tertiary granitoids from Thrace (northern Greece): Sr isotopic and petrochemical data, N. Jb. Mineral. Abh. 159 (1988) 113-135.

[40] Lilov P., Yanev Y., Marchev P., K/Ar dating of the eastern Rhodope Paleogene magmatism, Geol. Balc. 17 (1987) 49-58.

[41] Marchev P., Singer B., $^{40}Ar/^{39}Ar$ geochronology of magmatism and hydrothermal activity of the Madjarovo base-precious metal ore district, eastern Rhodopes, Bulgaria, in: Blundell D.J, Neubauer F., von Quadt A. (Eds), The Timing and Location of Major Ore Deposits in an Evolving Orogen, Geol. Soc. London Sp. Publ. 204, 2002, pp. 137-150.

[42] Singer B., Marchev P., Temporal evolution of arc magmatism and hydrothermal activity, including epithermal gold veins, Borovitsa caldera, southern Bulgaria, Econom. Geol. 83 (2000) 335-354.

[43] Pecskay Z., Elefteriadis G., Koroneos A., Soldatos T., Christofides G., K/Ar dating, geochemistry and evolution of the Tertiary volcanic rocks in Thrace, northeastern Greece, in: Eliopoulos D.G. *et al*. (Eds.), Mineral Exploration and Sustainable Development, 2003, Millpress, Rotterdam, pp.1229-1232.

[44] Ivanov, R. Stratigraphie und struktur der kristallins in den Ostrhodopen, Travaux sur Géologie de la Bulgarie, Série Géochemie 2 (1961) 69-119. (in Bulgarian, abstract in German).

[45] Kozhoukharov D., Kozhoukharova E., Papanikolaou D., Precambrian in the Rhodope massif, in: Zoubek, V. (Ed.), Precambrian in Younger Fold Belts, Willey, Chichester, 1988, pp. 723-778.

[46] Bonev N., Burg J-P., Ivanov Z., Mesozoic-Tertiary structural evolution of an extensional gneiss dome - the Kesebir-Kardamos dome, E. Rhodope, Bulgaria, (Int. J. Earth Sci. in review).

[47] Bonev N., Sillimanite-bearing migmatites from the Rhodope metamorphic complexes, southern Bulgaria: occurrence and implications for the tectono-metamorphic history, N. Jb. Geol.Paläont. Abh. 232 (2004) 57-75.

[48] Bonev N.G. Stampfli G.M., New structural and petrologic data on Mesozoic schists in the Rhodope (Bulgaria): geodynamic implications, C. R. Geoscience 335 (2003) 691-699.

[49] Marchev P., Singer B., Andrew, C., Hasson S., Moritz R., Bonev N., Characteristics and preliminary $^{40}Ar/^{39}Ar$ and $^{87}Sr/^{86}Sr$ data of the Upper Eocene sedimentary-hosted low-sulfidation gold deposits Ada Tepe and Rosino, SE Bulgaria: possible relation with core complex formation, in: Eliopoulos D.G. *et al*. (Eds.), Mineral Exploration and Sustainable Development, Millpress, Rotterdam, 2003, pp.1193-1196.

[50] Duffield W., Dalrymple G.B., The Taylor Creek Rhyolite of New Mexico: a rapidly emplaced field of lava domes and flows, Bull. Volcanology 52 (1990) 475-487.

[51] Renne P.R., Swisher C.C., Deino A.L., Karner D.B., Owens T.L., De Paolo D.J., Intercalibration of standards, absolute ages and uncertainties in $^{40}Ar/^{39}Ar$ dating, Chem. Geol. 145 (1998) 117-152.

[52] Singer B., Brown L.L., The Santa Rosa event: $^{40}Ar/^{39}Ar$ and paleomagnetic results from the Valles rhyolite near Jaramillo Creek, Jemez Mountains, New Mexico, Earth Planet. Sci. Lett. 197 (2002) 51-64.

[53] Harrison T. M., Duncan I., McDougall I., Diffusion of ^{40}Ar in biotite: temperature, pressure and compositional effects, Geochim. Cosmochim. Acta 49 (1985) 2461-2468.

[54] McDougall I., Harrison T.M., Geochronology and thermochronology by the $^{40}Ar/^{39}Ar$ method, Oxford University Press, Oxford, Second Edition, 1999, 269 p.

[55] Papadopoulos C., Geological Map of Greece 1:50 000. Map sheets Fere-Peplos-Enos-Maronia-Sappe-Kardamos-Virsini-Derio-Sufli-Didimoticho, 1982, IGME, Athens.

[56] Brun J-P., L'origine de dômes gneissiques: modèles at tests, Bull. Soc. Géol. France 25 (1983) 219-228.

[57] Lister G.S., Davis G.A., The origin of metamorphic core complexes and detachment faults formed during Tertiary continental extension in the northern Colorado river region, U.S.A., J. Struct. Geol. 11 (1989) 65-94.

[58] Brun J-P., Van Den Driessche J., Extensional gneiss domes and detachment fault systems: structure and kinematics, Bull. Soc. Géol. France 165 (1994) 519-530.

[59] Dutruge, G., Analyse petrostructurale de la localization de la deformation ductile dans les zones de cisaillement, PhD thesis, Universite Montpellier II, 1996, 234 p.

[60] Goranov A., Kozoukharov D., Boyanov I., Kozoukharova E., Geological map of Bulgaria 1:100 000. Map sheet Krumovgrad and Sape with explanatory note, 1995, 97 pp. (in Bulgarian).